

## Supplementary Information

### Temperature-dependence of magnetically-active charge excitations in Magnetite across the Verwey transition

M. Taguchi, A. Chainani, S. Ueda, M. Matsunami, Y. Ishida, R. Eguchi, S. Tsuda, Y. Takata, M. Yabashi, K. Tamasaku, Y. Nishino, T. Ishikawa, H. Daimon, S. Todo, H. Tanaka, M. Oura, Y. Senba, H. Ohashi, and S. Shin

#### A. Preparation of single crystal Fe<sub>3</sub>O<sub>4</sub>

The single crystals were annealed at around 1200 °C in an atmosphere of controlled mixture of CO and CO<sub>2</sub> in order to homogenize the composition of the specimen with different stoichiometry and to release internal strain. The stoichiometry of our single crystal is Fe<sub>3</sub>O<sub>4.002</sub> and it shows a very sharp transition at  $T_v = 123 \pm 0.05\text{K}$ . The composition of the samples was determined by thermogravimetry of single crystal chips. The annealing procedure and similar results have been reported in ref. [1].

#### B. Experimental details: MCD-HAXPES at BL15XU of SPring-8

The helical undulator provides circularly polarized x-rays with circular polarization ( $P_C$ ) ~0.99. In order to obtain the monochromatized x-ray with an energy resolution of ~50 meV at 5.95 keV, Si 111 double crystal monochromator and Si 333 channel-cut crystal were used, resulting in a reduction of  $P_C$  from 0.99 to 0.75. The incidence angle of x-rays and take-off-angle (TOA) of photoelectrons were set to 2° and 88° with respect to the sample surface. A magnetic field of 0.3 T was applied to the samples by a permanent magnet in the air before introducing into the analysis chamber attached to the electron analyzer (VG Scienta R4000-6kV). The magnetization direction was parallel to the sample surface. The Fermi level of gold was measured to calibrate the energy scale.

### C. Extended impurity Anderson model calculations

We used the extended impurity Anderson model with full multiplets including a well-screened feature from the electronic state near  $E_F$  to describe the spectra. The Slater integrals and the spin orbit coupling constants are calculated by Hartree-Fock code and are scaled down to 80% and 92%, respectively. The parameter values (in eV) are summarized in Table. S1. The parameters used in the calculations are: on-site Coulomb repulsion  $U$ , the attractive core-hole potential  $U_c$ , the charge transfer energy  $\Delta$ , the crystal field  $10Dq$ , the trigonal crystal field  $D_{trig}$  in the B-site, Fe3d – O2p hybridization  $V(e_g)$ . For the hybridization, we use the relations:  $V(t_{2g})=\sqrt{3}V(e_g)$  for  $T_d$  symmetry and  $V(e_g)=-2V(a_{1g})=-2V(e_g')$  for  $D_{3d}$  symmetry, respectively. We allow the 3d-band hybridization to be reduced by a factor  $R_C(= 0.8)$  in the presence of the core hole and enhanced by a factor  $1/R_V(= 1/0.9)$  in the presence an extra 3d electron. We introduce the state  $C$  on the top of valence band and define the parameter:  $\Delta^*$  - the charge transfer energy between Fe 3d and  $C$ . An effective coupling parameter  $V^*$ , for describing the interaction strength between the Fe 3d and coherent state is introduced, analogous to the Fe3d - O2p hybridization. We assume rectangular bands for O2p and coherent state  $C$  of width  $W_O$  and  $W_C$ , respectively.

The precise XRD studies indicate the existence of small charge modulation below Verwey transition.[2-4] For example, Blasco *et al.* have shown ten different environments in the octahedral B-site, resulting ten different valences between 2.53 and 2.84. The valences of Fe(B1a), Fe(B1b'), Fe(B4'), Fe(B3) iron atoms were approximately 2.5 and the valences of Fe(B4), Fe(B1b) were about 2.7. The remaining B-site Fe atoms show more than 2.8 valences. Therefore, three types of parameter sets (*i.e.* Fe<sup>2.4~2.5+</sup>-like, Fe<sup>~2.7+</sup>-like and Fe<sup>2.8~2.94+</sup>-like) were used for the B-sites in the present calculations.

**Table S1.** Estimated parameter values for high and low temperature phases of Fe<sub>3</sub>O<sub>4</sub>.

	High temperature phase (in eV)									
	$\Delta$	$\Delta^*$	$U$	$U_c$	$V(e_g)$	$V^*(e_g)$	$10Dq$	$D_{trig}$	$W_O$	$W_C$
<b>B-site <math>D_{3d}</math></b>	5.5	1.1	7.0	7.7	3.3	0.66	1.22	0.5	8.0	0.5
<b>A-site <math>T_d</math></b>	4.5	1.0	7.0	7.7	1.1	0.12	-2.0		8.0	0.5

**Low temperature phase (in eV)**

	$\Delta$	$\Delta^*$	$U$	$U_c$	$V(e_g)$	$V^*(e_g)$	$10Dq$	$D_{trig}$	$W_O$	$W_C$
B-site ( $\text{Fe}^{2.4\sim 2.5+}$ like) $D_{3d}$	5.2	1.1	7.0	7.7	3.6	0.576	1.22	0.5	8.0	0.5
B-site ( $\text{Fe}^{2.7+}$ like) $D_{3d}$	5.5	1.1	7.0	7.7	3.3	0.66	1.22	0.5	8.0	0.5
B-site ( $\text{Fe}^{2.8\sim 2.94+}$ like) $D_{3d}$	6.0	1.1	7.0	7.7	3.3	0.528	1.22	0.5	8.0	0.5
<b>A-site <math>T_d</math></b>	4.5	1.0	7.0	7.7	1.0	0.088	-2.0		8.0	0.5

**D. The details of the line-shape analysis of the temperature-dependent valence band PES**

Following the analysis by Kobayashi *et al.*[5], we have performed the same type of line-shape analyses for the temperature dependent valence band PES of single crystal  $\text{Fe}_3\text{O}_4$ . For the low temperature insulating phase, the line-shape was assumed to be of the form  $I(E_B) = a_1(E_B - E_0)\theta(E_B - E_0)$  in order to represent the finite gap  $E_0$ , where  $\theta(E_B - E_0)$  is the step function. In the high temperature metal phase, we assumed  $I(E_B) = (a_1 E_B + a_0)f(E_B, T)$ , where  $f(E_B, T)$  is the Fermi-Dirac distribution function at  $T$ .  $a_0$  and  $a_1$  were treated as adjustable parameters.

**E. O  $1s$  HAXPES spectra of single crystal  $\text{Fe}_3\text{O}_4$**

Figure S1 shows the temperature dependence of O  $1s$  core-level HAXPES spectra. The asymmetry due to electron-hole pair shake-up (the Doniach-Šunjić line shape) is clearly observed in the high temperature phase and gets reduced on decreasing temperature below  $T_V$ . This is another indication of the gapless electronic state of the high temperature phase.

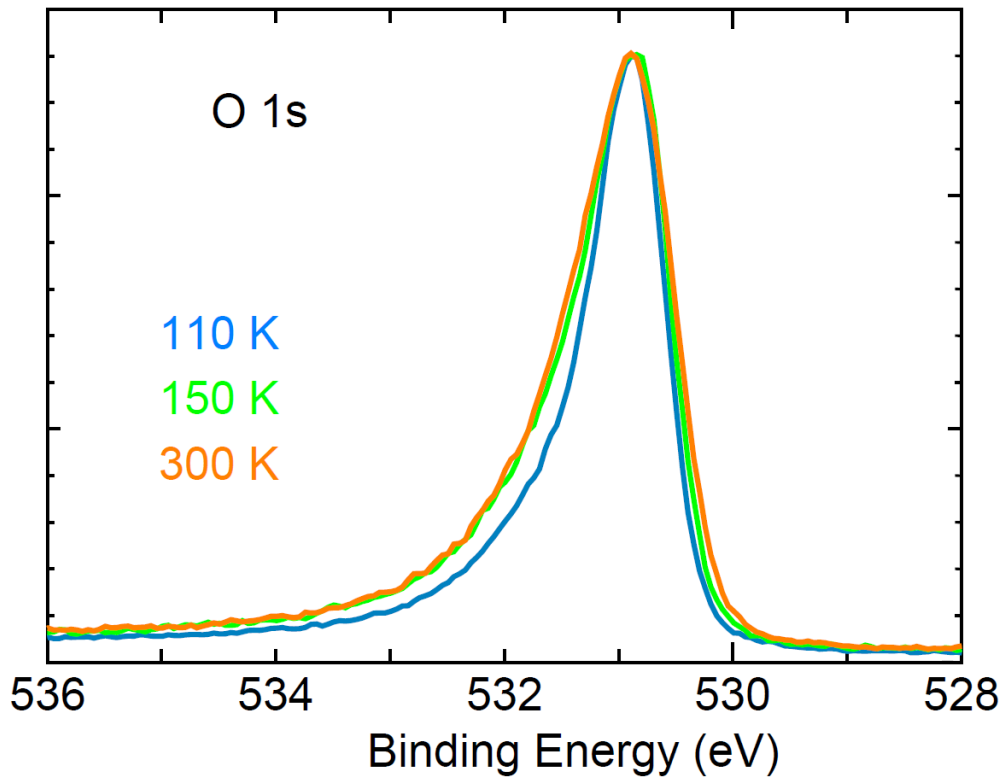


**Fig. S1.** O *1s* core-level HAXPES spectra of single crystal Fe<sub>3</sub>O<sub>4</sub> across the Verwey transition using hard x-ray ( $h\nu = 7.94$  keV).

- 
- [1] S. Todo, K. Siratori and S. Kimura, *J. Phys. Soc. Jpn.* **64**, 2118 (1995).
  - [2] J. P. Wright, J. P. Attfield, and P. G. Radaelli, *Phys. Rev. Lett.* **87**, 266401 (2001).
  - [3] J. Blasco, J. Garcia and G. Subias, *Phys. Rev. B* **83**, 104105 (2011).
  - [4] M. S. Senn, J. Wright, and J. P. Attfield, *Nature* **481**, 173 (2012).
  - [5] K. Kobayashi, T. Susaki, A. Fujimori, T. Tonogai, and H. Takagi, *Europhys. Lett.* **59**, 868 (2002).